Abdominal Radiology (2019) 44:3800–3810
https://doi.org/10.1007/s00261-019-02085-1

SPECIAL SECTION : UROTHELIAL DISEASE

Update on MR urography (MRU): technique and clinical applications

Jorge Abreu-Gomez[1] · Amar Udare[1] · Krishna P. Shanbhogue[2] · Nicola Schieda[3]

Published online: 1 June 2019

Abstract
Magnetic resonance imaging of the upper tract (pyelocalyces and ureters) or MR Urography (MRU) is technically possible and when performed correctly offers similar visualization of the upper tracts and for detection of non-calculous diseases of the collecting system similar specificity but with lower sensitivity compared to CTU. MRU provides the ability to simultaneously image the kidneys and urinary bladder with improved soft tissue resolution, better tissue characterization and when combined with assessment of the upper tract, a comprehensive examination of the urinary system. MRU requires meticulous attention to technical details and is a longer more demanding examination compared to CTU. Advances in MR imaging techniques including: parallel imaging, free-breathing motion compensation techniques and compressed sensing can dramatically shorten examination times and improve image quality and patient tolerance for the exam. This review article discusses updates in the MRU technique, summarizes clinical indications and opportunities for MRU in clinical practice and reviews advantages and disadvantages of MRU compared to CTU.

Keywords Magnetic resonance imaging · Urography · Urothelium

Introduction

Imaging of the upper tracts (e.g. the collecting system which includes the pyelocalices and ureters) is a common indication in clinical practice for evaluation of: patients with hematuria, a dilated or potentially obstructed collecting system and those patients with documented urothelial cell carcinoma (UCC) or other tumors of the urinary tract which require staging or re-staging examinations [1–3]. Imaging of the upper tracts is typically performed with CT Urography (CTU) in most clinical practices throughout the world due to shorter examination times, improved efficiency and patient throughput, better availability and decreased technical and interpretative complexity compared to MR Urography (MRU) [4–6]. Nevertheless, MRU (when technically optimized) offers similar visualization of the ureters compared to CTU and for detection of non-calculous diseases of the collecting system has been shown to be as specific as CTU albeit with lower sensitivity [7, 8]. MRU is non-ionizing and presents an ability to image the collecting systems, as well as, the kidneys and urinary bladder simultaneously as a comprehensive "one-stop-shop" examination [9]. Advances in MR imaging techniques including: parallel imaging, motion compensation and compressed sensing may dramatically shorten examination times improving image quality and patient tolerance for the MRU examination. This review article discusses the MRU technique (including technological advances), clinical indications and accuracy of MRU and debates advantages and disadvantages of MRU compared to CTU.

Technique

A comprehensive MRU requires anatomic coverage of the kidneys, urinary bladder and the collecting system in its'

✉ Nicola Schieda
nschieda@toh.on.ca

Jorge Abreu-Gomez
jabreugomez@toh.on.ca

Amar Udare
audare@toh.on.ca

Krishna P. Shanbhogue
Krishna.Shangbhogue@nyulangone.org

[1] Department of Medical Imaging, The Ottawa Hospital, The University of Ottawa, Ottawa, ON, Canada

[2] Department of Radiology, NYU Langone Health, New York, USA

[3] The Ottawa Hospital, The University of Ottawa, 1053 Carling Avenue, Ottawa, ON K1Y 4E9, Canada

entirety including the pyelocaliceal system and ureters. The craniocaudal distance required to cover all of the anatomy of the urinary tract poses a technical challenge for many MRI systems [9]. Most abdominal and pelvic MRI surface coils offer an imaging field of view (FOV) of up to 40 cm [10] which may be too small to cover the entire urinary tract simultaneously. A simple solution, though time consuming and somewhat impractical, is to cover the upper abdomen and pelvis separately. This requires moving the surface coil in between acquisitions and necessitates re-localization between stations [11, 12]. Dynamic contrast-enhanced (DCE)-MRI can only be performed once using this set-up and can cover either the upper abdomen or the pelvis but not both. Vendors have proposed various solutions to overcome this challenge, and include: larger surface coils with wider useable FOV, integrated surface coils which enable linking of adjacent coils expanding the useable FOV and continuously moving table (CMT) MRI [11, 12]. Even when coverage is possible, acquisition times can be prohibitive if modifications to existing protocols are not performed. One simple strategy to reduce acquisition time is to image in the coronal (as opposed to the axial) plane to reduce the number of slices required to achieve adequate coverage. Increasing slice thickness or reducing resolution through reductions in the number of phase-encoding steps can also shorten acquisition times to improve coverage. Other techniques which may be used to reduce examination times will be discussed later.

A basic MRU examination typically includes T2-weighted (T2W) imaging obtained at standard and very long echo times (TE ~ 90 and > 500 ms, respectively), T1-weighted (T1W) images acquired with dual-echo chemical shift imaging (CSI) and with fat suppression (FS) before and after gadolinium administration. When gadolinium enhanced images are acquired through DCE-MRI and when diffusion weighted imaging (DWI) is added to a basic MRU protocol, a "multi-parametric" MRU is achieved [9]. Delayed T1W gadolinium enhanced urographic phase images complete the protocol. Our institutional MRU protocol is summarized in Table 1.

Components of multi-parametric MR urography (MRU)

Patient preparation

Two key components which are required to achieve a good quality MRU are adequate hydration status and patient diuresis. The patient should be well hydrated before MRU. If there is no contraindications (e.g. congestive heart failure, fluid restriction), 250–500 ml of IV saline may be administered at least 30 min before the start of imaging. The urinary bladder (UB) should be half full at the beginning of the examination given that an overdistended UB could result in unwanted motion artifact, cause patient discomfort or potential delays if, for example, the patient needs to void during the examination [9, 12]. Alternatively, a completely collapsed UB is also not ideal since underdistention can also simulate pathology [13].

T2-weighted imaging (fluid sensitive MRU)

T2W images for MRU use the intrinsically high signal intensity of the urine for image contrast. Single-shot half-Fourier fast or turbo spin echo (ssFSE/HASTE) T2W images are routinely performed when imaging the kidneys and ureters [3]. TE times may vary slightly by system but are generally performed with moderate T2 weighting (e.g. TE 60-120 ms) which provides good contrast between the kidneys, collecting systems and disease [12]. Advantages of ssFSE/HASTE compared to conventional FSE/TSE are mainly shorter acquisition times and the ability to freeze motion in any single image to reduce artifact. Disadvantages include lower spatial resolution and image blur (due to the extended echo-train) and when staging a primary urothelial cell malignancy in the urinary bladder 2D or 3D TSE/FSE are preferred. A series of coronal thick-slab fat-suppressed heavily T2-weighted (e.g. TE > 500 ms) MRCP-type ssFSE/HASTE images can be acquired in 2–3 s to provide a broad overview of the collecting systems and potentially differentiate areas of pathological ureteric narrowing/stricturing from ureteric peristalsis [9]. Alternatively, heavily T2W MRU images can be obtained as a free-breathing or respiratory triggered 3D acquisition which can be later partitioned into thin slices and reconstructed into any imaging plane [14]. An advantage of T2W MRU is that it does not require gadolinium. In cases of a moderately to severely obstructed collecting system, T2W MRU may be the best method to detect a collecting system abnormality since the urine within the dilated collecting system provides excellent inherent image contrast and excretory phase urographic images in patients with a dilated collecting system may be poor due to reduced excretion of contrast, lower opacification and mixing effects between gadolinium and urine in a dilated system, Fig. 1.

T1-weighted imaging (gadolinium-enhanced MRU)

Gadolinium enhanced T1W MR urography is dependent on the renal excretory function of the patient [15]. In a patient with poor or absent renal function, an insufficient amount of gadolinium may be excreted. In these cases T2W MRU may be the only alternative. Gadolinium within the collecting systems expectedly shortens the T1 relaxation time of urine with resultant increased signal intensity of urine on T1W images; however, as gadolinium concentrates in the collecting systems an eventual paradoxical loss of signal

Table 1 Example MRU protocol performed at our institution at both 1.5 and 3 Tesla

Imaging plane	T2W Single-shot Half-Fourier Turbo spin echo (ss-TSE/FSE[a])		T1W Chemical shift (IP+OP[b]) 2D GRE	T1W FS 3D Gradient recalled echo (GRE)[c]	T2W TSE/FSE	Heavily T2W –MRCP-type ss-TSE/FSE	Post-Gadolinium[d] Dynamic FS 3D GRE	Diffusion weighted imaging[e]	Post-Gadolinium[f] FS 3D GRE Urogram
	Coronal	Axial	Axial	Axial	Axial and Coronal	Coronal	Axial	Axial	Coronal
Coverage	Abdomen and Pelvis	Abdomen Pelvis with overlap	Abdomen	Abdomen and Pelvis with overlap	Pelvis only	Abdomen and Pelvis	Abdomen and Pelvis (delay)	Abdomen and pelvis with overlap	Abdomen and pelvis
Fat Suppression	N/A	N/A	N/A	Spectral adabiatic inversion recovery	N/A	Spectral adabiatic inversion recovery	Spectral adabiatic inversion recovery	Spectral adabiatic inversion recovery	Spectral adabiatic inversion recovery
Physiology[g]	Breath-hold	Breath-hold	Breath-hold	Breath-hold	Free-breathing	Breath-hold	Breath-hold	Breath-hold	Breath-hold
Volumetry	2-Dimensional	2-Dimensional	2-Dimensional	3-Dimensional	2-Dimensional	2-Dimensional	3-Dimensional	2-Dimensional	3-Dimensional
Slice thickness (mm)	6	5	5	2	4	60	5	6	30
Matrix	218×320	195×320	154×256	144×320	320×320	512×333	320×144	142×115	384×307
Field of View (mm)	420×357	360×274.5	400×300	350×262.5	300×300	350×350	350×262	400×400	370×370
TE/TR (msec)	90/2000	93/2000	2.35/172[g] 4.87/172	1.46/4.30	124/8440	985/4500	1.46/4.3	74/4600	875/4500
Flip Angle (degrees)	90	150	70	12	128	150	80	N/A	180
Bandwidth (Hz)	679	781	390	490	265	264	490	1446	130
Acceleration	2	2	2	0	0	0	0	2	2
Number of signals averaged	1	1	1,2[h]	1	1	1	1,4,6[i]	3	1

Typical examination time is between 40 and 50 min

MRI performed on 4 clinical MR systems including at 1.5 Tesla (Symphony and Aera, Siemens Medical, Malvern PA) and at 3T (TRIO, Siemens Medical, Malvern PA and Discovery 750W, General Electric Health Care, Milwaukee WI). Combined surface coils with activated spine array

[a]Single-shot Turbo Spin Echo or Fast Spin Echo; HASTE (Siemens Medical, Malvern PA) and ssFSE (General Electric Medical, Milwaukee WI)

[b]In-Phase and Opposed-Phase

[c]VIBE (Siemens Medical, Malvern PA) and LAVA (General Electric Medical, Milwaukee WI)

[d]4 phases acquired dynamically starting with the cortico-medullary phase timed empirically at 35 s, followed by the nephrographic phase at 120 s post-injection. Axial, coronal and sagittal delayed sequences are also performed. Gadolinium injected at a concentration of 0.1 mmol/kg using gadobutrol (Gadovist, Bayer Inc. Toronto, ON) at a rate of 3 mL/sec. IV Furosemide injected just prior to gadolinium administration

[e]Diffusion weighted imaging performed with spectral fat suppression echo-planar imaging with tridirectional motion probing gradients and *b* values of 0, 600 mm/s^2 with automatic apparent diffusion coefficient map generation using mono-exponential curve fitting

[f]Urographic phase performed first at 8 min

[g]All breath-holds performed with end expiration

[h]Number of signals averaged partitioned by *b* value

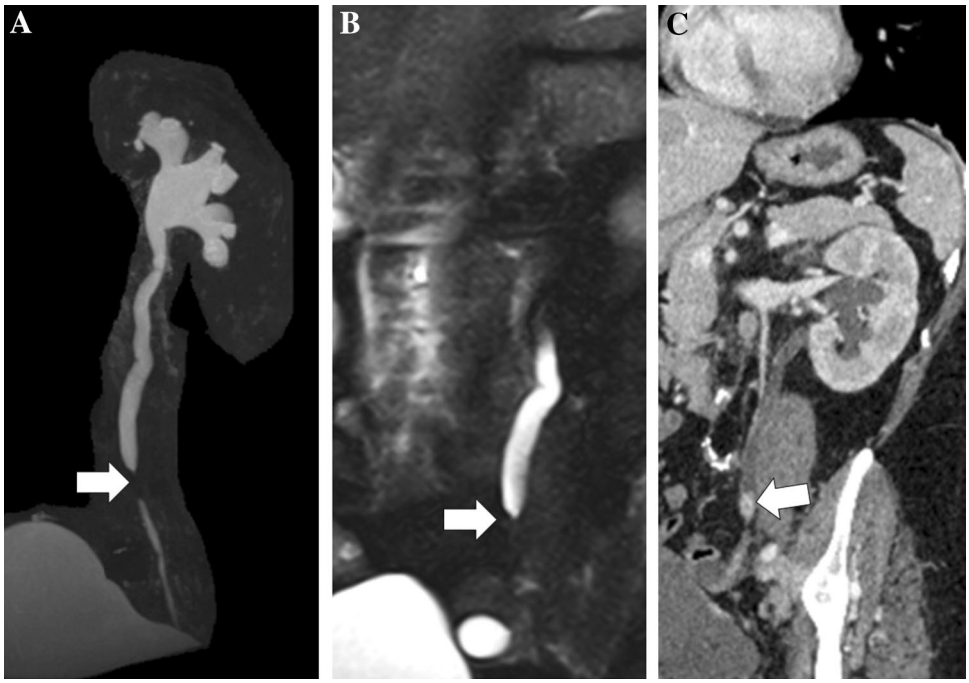

Fig. 1 54-year-old woman with history of colorectal cancer who underwent MR urography for further evaluation of a dilated collecting system detected on ultrasound (not shown). **a** Coronal maximum intensity projection (MIP) image from a thick-slab fat-suppressed (FS) heavily T2-weighted (T2W) 3D fast spin-echo (FSE) MR image [T2 MR urography (MRU)] shows a moderately dilated left collecting system with an abrupt narrowing of the left distal ureter (arrow). **b** Coronal fat suppressed T2-weighted (T2W) single-shot fast spin-echo (ssFSE) MR image further identifies the abrupt narrowing of the left distal ureter (arrow) due to a filling defect causing convex superior margins. Gadolinium was not administered due to poor excretory function. **c** Follow-up oblique coronal reformatted image from a contrast-enhanced CT shows an enhancing lesion (arrow) in the left distal ureter at the site of obstruction. Metastatic colon cancer was diagnosed at subsequent ureteroscopic biopsy

intensity on T1W images occurs due to susceptibility (T2*) effects which overwhelm T1 shortening [16]. The loss of signal intensity may limit adequate assessment of the collecting systems either obscure pathologic findings or simulating a filling defect, Fig. 2 [9, 12]. This is a fundamental difference comparing CTU and MRU, where in the former longer delays result in improved opacification of the collecting systems, whereas, in the latter may render the study non-diagnostic. To minimize signal intensity loss from susceptibility effects, adequate gadolinium dilution is required.

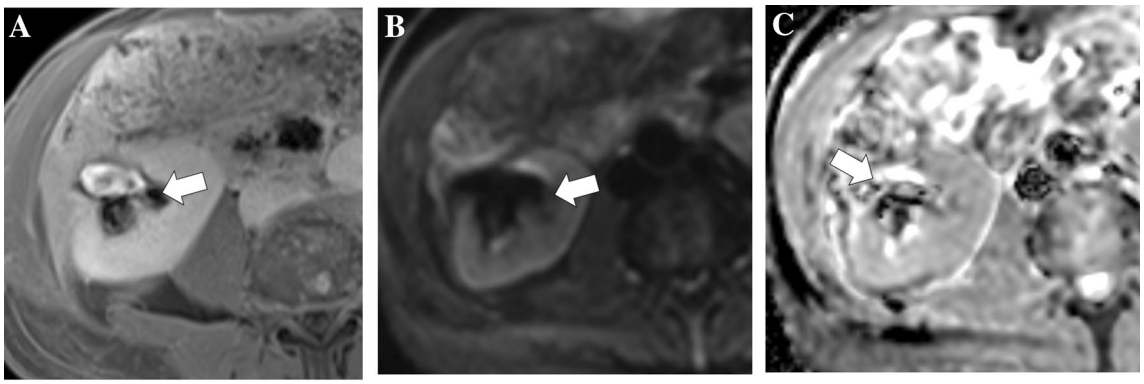

Fig. 2 25-year-old woman undergoing MRU for evaluation of hematuria. **a** Axial T1-weighted (T1W) FS gradient-recalled echo (GRE) MR image obtained during the urographic phase shows blooming artifact (arrows) in the renal sinuses due to concentrated gadolinium, limiting evaluation. Artifact is also simulating filling defects within the renal pelvis. **b, c** Axial FS echo-planar diffusion-weighted image (DWI) with b value of 600 s/mm^2 and ADC map image show T2* artifact (arrows) in renal sinus with a complete signal void and geometric warping due to concentrated gadolinium in renal hilum

This can be achieved either by increasing the amount of volume in the collecting system (through the administration of IV fluids) or by the administration of diuretics (e.g. IV Furosemide injected at doses of 10–20 mg) or both [5, 9]. Alternatively, reducing the dose of administered extracellular GBCA or using a combined extracellular/hepatobiliary contrast agent (e.g. Gadoxetic acid, marketed as Primovist in Canada or Eovist in the United States] can also be performed to dilute the concentration of gadolinium in the collecting systems [17, 18], Figs. 3 and 4.

Functional imaging [diffusion-weighted imaging (DWI) and dynamic contrast enhanced (DCE)-MRI]

DCE-MRI is routinely obtained in the corticomedullary and nephrographic phases for the detection, characterization and staging of renal parenchymal neoplasms [10, 19]. Tumors of the pyelocalyceal system and ureters, mainly urothelial cell carcinomas (UCC) can be identified after contrast administration as enhancing lesions corresponding to filling defects on T2W [20]. To our knowledge the use of DCE-MRI for upper tract lesion characterization has not been formally reported. In a study by Kim et al., a time-resolved DCE-MRI was able to diagnose areas of ureteric peristalsis [21]. Future studies may evaluate upper tract neoplasms with DCE-MRI, which may be now technically possible due to recent technological advancements which enable more rapid or motion-compensated DCE-MRI of the upper abdomen, discussed below.

Diffusion weighted imaging (DWI) has been incorporated into most abdominal and pelvic MRI protocols and has an important role in renal and urinary bladder mass evaluation [22–25]. A comprehensive explanation of DWI, as it applies to oncologic imaging, is beyond the scope of this manuscript but has been described elsewhere [26–29]. DWI has been investigated and shown to be useful for the detection of upper tract tumors [22, 30, 31] and also for prediction of histopathological grade and T stage [32]. It is important to emphasize that DWI, when imaging the collecting systems, requires the use of a high *b* value image (e.g. ≥ 600 mm/s^2) to suppress the unwanted signal from urine and emphasize the abnormal signal from upper tract tumors, Fig. 3. Through

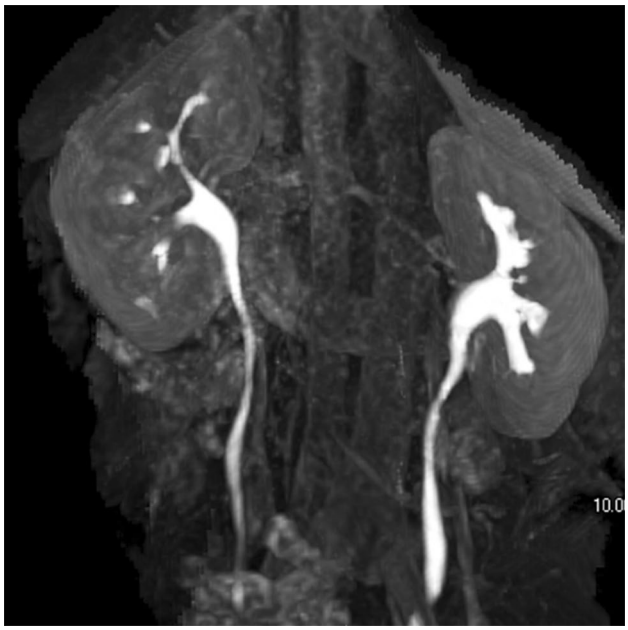

Fig. 4 60-year-old male who underwent MRU for evaluation of colorectal cancer metastases and hematuria using a mixed extracellular–hepatobiliary phase contrast agent (Gadoxetic acid, Bayer Pharmaceuticals). Coronal MIP image shows excellent opacification of the pyelocalyceal systems and upper ureters without significant susceptibility artifact. The dual excretion of the gadolinium and lower administered dose results in sufficient dilution in the urinary tract to prevent unwanted susceptibility artifact

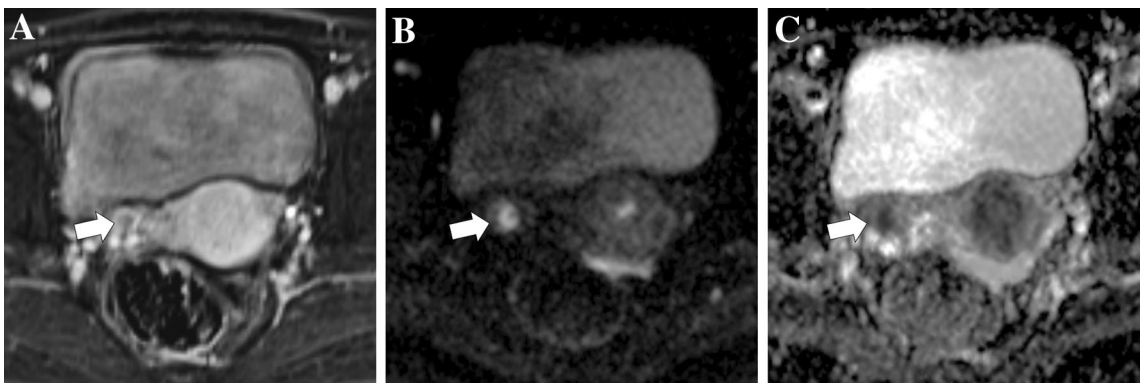

Fig. 3 54-year-old male with right distal ureteric urothelial carcinoma. **a** Axial T1W FS GRE MR image in the urographic phase shows a filling defect in the opacified right distal ureter (arrow). **b** and **c** Axial DWI (*b* value, 600 s/mm^2) and ADC images show marked restricted diffusion in the lesion (arrows). Note that at high *b* value DWI the signal intensity of the urine decreases (due to unrestricted diffusion), whereas the signal intensity of the tumor remains bright improving lesion detection

the use of commercially available software, high *b* value images can be calculated or extracted from a DWI acquisition of low and intermediate *b* values which has been shown to not only shorten examination times but also improve contrast to noise ratio when imaging at very high *b* values in the prostate [33, 34]. When combining a high *b* value acquisition with a low (± intermediate) *b* value, apparent diffusion coefficient (ADC) map images are obtained which highlight tumors as having low signal intensity contrasted to hyperintense urine which shows T2 shine-through effects. It is important to recognize that most clinical DWI in the abdomen and pelvis continues to be acquired using single-shot echo-planar imaging (EPI) techniques which are extremely sensitive to susceptibility artifact. Therefore, DWI should be acquired prior to administration of gadolinium to minimize susceptibility artifact from gadolinium in the collecting systems which may render DWI non-diagnostic [9], Fig. 5.

Adding DCE-MRI with DWI to an MRU examination results in a full multi-parametric MRU. Though multi-parametric MRU is not well studied, there are instances where the combination of imaging findings may improve diagnostic accuracy. For example, an important scenario arises in clinical practice when a central/hilar tumor involving the pyelocalyceal system is identified on imaging. In this context, the two leading considerations are a hilar renal cell carcinoma (RCC, most frequently clear cell subtype) and UCC. Differentiating between these two diagnoses preoperatively is important. Management for clear cell RCC is accomplished by nephrectomy or complex partial nephrectomy [35], whereas for UCC reference standard management for high grade disease is with nephroureterectomy and resection of the bladder cuff with alternative strategies reserved for selected patients who are poor operative candidates or require preservation of renal function [36]. Pre-operative histological diagnosis may be challenging due to the deep hilar location of these central tumors which may be difficult to biopsy percutaneously or endoscopically [37]. Studies have evaluated the ability of MRI to differentiate between hilar clear cell RCC and UCC with good results [38]. Clear cell RCC typically show increased T2W signal intensity, may contain microscopic fat which can be depicted on T1W in- and opposed-phase dual-echo GRE images [39], show modest restricted diffusion and enhanced avidly and heterogeneously in the corticomedullary phase with washout kinetics. Conversely, UCC show low T2W signal intensity, no microscopic fat, marked restricted diffusion and progressive fairly homogeneous low enhancement, Figs. 5 and 6.

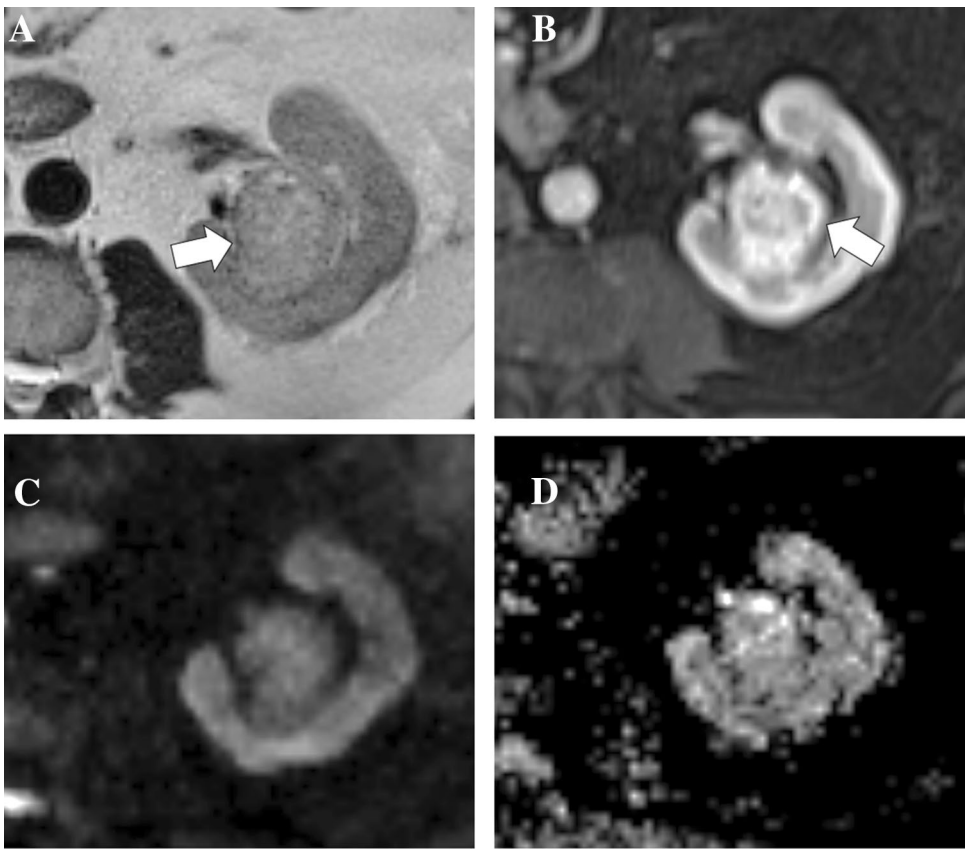

Fig. 5 70-year-old male with clear cell renal cell carcinoma (RCC) extending into the renal sinus mimicking a urothelial cell carcinoma. **a** Axial T2W ssFSE image shows a well circumscribed T2W hyperintense mass in the renal sinus of the left kidney. **b** Axial FS T1W GRE MR image in the corticomedullary phase of enhancement shows avid heterogeneous enhancement in the mass (arrow) **c** and **d** Axial DWI (*b* value, 600 s/mm^2) and ADC map images show only mild restricted diffusion

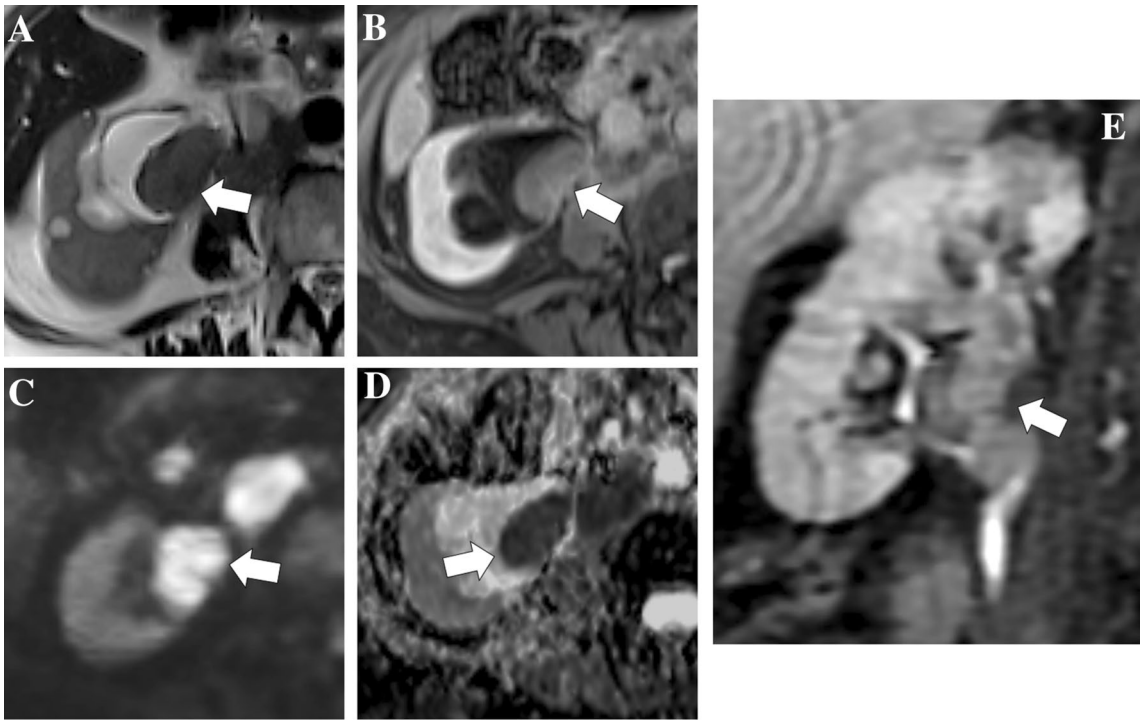

Fig. 6 62-year-old woman with urothelial carcinoma involving the right renal hilum. **a** Axial T2W ssFSE image shows a homogeneously T2W hypointense mass lesion centered in the right renal pelvis. **b** Axial FS T1W GRE MR image obtained in the nephrographic phase of enhancement shows mild homogenous enhancement in the mass (arrow). **c** and **d**. Axial DWI (*b* value, 600 s/mm2) and ADC map images show marked restricted diffusion in the mass. **e**. Coronal FS T1W GRE MR image in the urographic phase shows the mildly enhancing mass lesion as a filling defect in the renal pelvis

Advanced Imaging techniques and potential applications for MRU

Recent technological advances in abdominal and pelvic MRI have attempted to significantly shorten examination times or acquire good diagnostic quality free-breathing images using motion correction techniques. These techniques have been discussed in detail in a recent review article summarizing advances in gadolinium-based contrast agent imaging in the genitourinary tract [40]. Briefly, through advanced parallel imaging and compressed sensing techniques, acquisition times can be shortened substantially. Both methods shorten examination times by reducing the number of phase-encoding steps (undersampling k-space) and then reconstruct a final image while attempting to maintain image quality and minimize noise and other artifacts. These reductions in acquisition times can be used in MRU to achieve shorter breath-holds (improving patient tolerance), greater anatomic coverage in the slice selection axis or can be used to improve spatial resolution. Alternatively, novel prospective or retrospective motion-compensated imaging techniques could enable a free-breathing urographic phase acquisition with 3D T1W gradient recalled echo sequences at isotropic resolution. When these free-breathing motion-compensated techniques are combined with advanced parallel imaging and compressed sensing, completely free-breathing studies including DCE-MRI are now technically possible [40]. With application of machine-learning techniques, historical shortcomings of MRU including longer acquisition times and reduced patient tolerance may become even less problematic in the future.

Texture analysis of medical images is an emerging field which has drawn particular attention for genitourinary application [21, 36–38]. Texture analysis offers the ability to quantitatively assess for differences in pixel values which are not perceptible to the human eye and has been preliminarily studied in urothelial cell carcinomas of the upper tract and urinary bladder on CT and MRI [42–45]. Further, larger scale studies are needed to validate preliminary results and apply texture analysis to machine-learning algorithms for automated detection and characterization of upper tract disease.

Clinical applications of MRU

Iodinated contrast allergy and other concerns

Patients with known severe allergic reactions to iodinated contrast material alternatively can be imaged with gadolinium-enhanced MRU [1, 3] to avoid the potential risks related to re-exposure of iodinated contrast media in the context of a prior severe allergic reaction. Gadolinium-enhanced or T2W MRU may also be preferred to CTU in patients where iodinated contrast media are considered less desirable (e.g. in patients with compromised renal function, on dialysis or with renal transplants). Moreover, in patients whose condition (e.g. pregnancy) or preference is to avoid all forms of contrast media, T2W-MRU offers an alternative imaging strategy avoiding contrast media altogether [39].

Radiation

MRU is considered the first line examination in young patients with complex congenital abnormalities or warranting multiple serial follow-up examinations [12]. Additionally, T2W MRU is also recommended in the evaluation of obstructive uropathy in pregnant patients [1]. As model based and artificial intelligence based iterative reconstruction techniques continue to lower radiation dose on CT [46–48], radiation is less of a concern in clinical practice; however, in selected patients, MRU provides an excellent alternative imaging modality.

Ureteric calculi

MRI is relatively insensitive for the detection of renal calculi compared to CT [49–51]. Currently, patients with suspected or documented urolithiasis requiring imaging should undergo low-dose unenhanced CT rather than MRU [12]. In unsuspected patients with urolithiasis undergoing MRI or MRU, secondary findings of significant calculous disease such as: hydroureteronephrosis, a delayed nephrogram, renal engorgement, perinephric stranding or fluid and urothelial thickening may be findings which herald an underlying calculus as a potential cause. Typical findings of a renal calculus on MRI include a persistent filling defect on T2W or excretory MRU without enhancement [3] which may or may not show susceptibility artifact comparing signal intensity on longer TE in-phase to shorter TE-opposed-phase images. In the absence of obstruction, non-obstructing renal calculi are commonly overlooked on MRI.

Dilated and potentially obstructed collecting system

MRU is considered more sensitive and specific for noncalculous causes of urinary tract obstruction than unenhanced CT [52]. A variety of intrinsic and extrinsic causes for urinary tract obstruction can be encountered on MRU [4, 20, 53]. Benign strictures of the ureters can be due to adjacent abdominal and pelvic inflammatory processes such as appendicitis, Crohn's disease or endometriosis or result from previous surgical or radiotherapy. Benign strictures are typically smoothly tapering and not associated with a soft tissue mass [12], whereas malignant strictures may present with an enhancing mass at the site of ureteral obstruction, abrupt change in caliber and a meniscus at the tumor–urine interface. Differentiation between benign and malignant strictures can be difficult when urothelial carcinoma presents as concentric ureteral thickening and enhancement [19]; DWI and in particular ADC measurements could be useful additional features for imaging differentiation; however, differentiating malignant from benign ureteric lesions with wall thickening remains a challenge [54]. It is important to differentiate strictures from normal ureteric peristalsis which can be accomplished readily at MRU using a series of thick-slab heavily T2W MRU single-shot ssFSE/HASTE images or less commonly using time-resolved DCE-MRI [21].

Upper tract neoplasms

UCC represents approximately 90% of primary pelvicalyceal malignancies with squamous cell carcinoma accounting for the remaining 10% [55]. A hallmark of UCC is high recurrence rates and multiplicity of disease, requiring strict surveillance of the urothelium [56]. UCC is typically divided into upper urinary and lower urinary tract tumors, based on differences in the natural history of disease and treatment approaches. Upper tract UCC can be seen in nearly 2–4% of patients with bladder cancer; therefore, imaging surveillance of the upper urinary tract is considered a key factor in the management of bladder tumors [57, 58]. On the other hand, approximately 40% of patients with upper tract UCC will develop a bladder cancer, highlighting the importance of bladder surveillance during the oncologic follow up of patients with upper tract UCC [56, 59]. As discussed above, multi-parametric MRU can reliably differentiate between UCC involving the pyelocalyceal system and central or hilar RCC. Ureteric UCC can be diagnosed at MRU when noting a filling defect or mass in the ureter on T2W or excretory phase T1W MRU which enhances on early DCE-MRI, Fig. 7.

Infection

Urinary tract infection (UTI) can occur anywhere in the urinary tract from the urethra to the kidney and is most

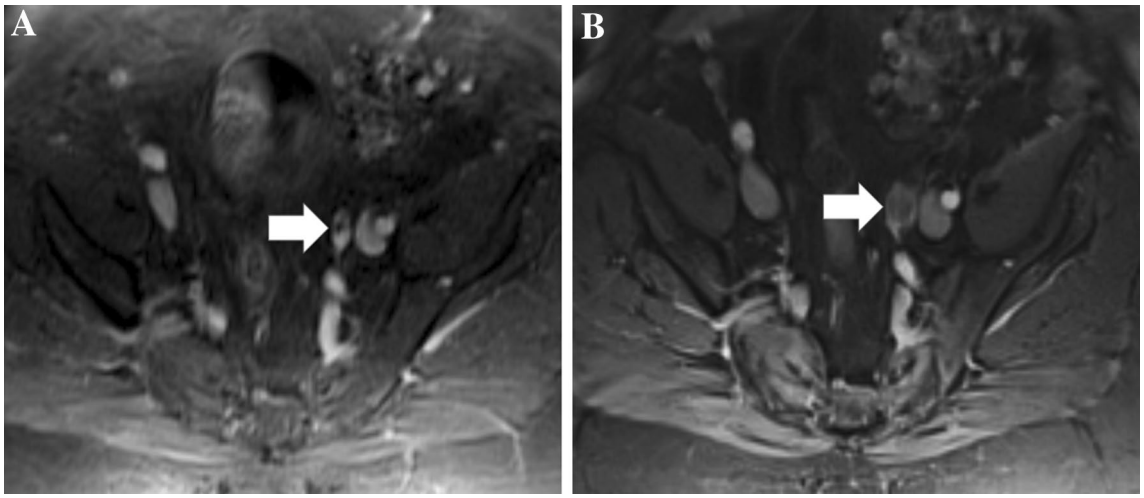

Fig. 7 67-year-old woman with history of urinary bladder urothelial cell carcinoma status post-transurethral resection of bladder tumor undergoing MRU for surveillance of disease in the upper tracts. **a** Axial FS T1W GRE MR image obtained in the urographic phase shows a 4 mm filling defect in the opacified left distal ureter (arrow). The lesion was not prospectively reported. **b** Axial FS T1W GRE MR image obtained in the urographic phase in the same patient on a 2-year follow-up MRU shows the lesion has grown and now fills the distal ureter measuring 16 mm (arrow). Ureteric UCC was confirmed at ureteroscopic biopsy

commonly due to bacterial infections. Imaging is generally not performed for the majority of UTI; however, can be crucial when assessing for complications related to infection. In pregnant patients, MRI is considered the best imaging modality for the evaluation of complicated UTI [60]. MRI can be especially useful for diagnosis and follow-up of renal abscesses [60]. It is important to highlight the limitation of MRI, compared to CT, for the detection of calculi (in the context of a suspected septic stone) and air (in the context of emphysematous pyelitis and pyelonephritis).

Retroperitoneal masses which may be extrinsic to the collecting systems

A wide variety of retroperitoneal benign and malignant conditions can secondarily involve the ureters and renal pelvis resulting in hydroureteronephrosis either from mass effect/compression or frank invasion. To our knowledge, CT and MRI have not been directly compared for assessing retroperitoneal disorders but, in our opinion, are comparable in terms of diagnostic accuracy. Retroperitoneal fibrosis is an uncommon fibrotic reaction characterized by the development of a fibrous plaque in the retroperitoneum, frequently surrounding the ureters and causing obstruction [61, 62]. The disease progresses from active inflammation to fibrous scarring [63, 64]. On imaging, as the maturation process evolves from the periphery to the center, the lateral edges of the lesion tend to be hyperintense on T2W and enhancing after contrast administration, whereas the central areas tends to be more fibrotic with low signal intensity on T2W [64]. Assessment of disease activity is relevant for planning of further medical or surgical therapy [65]. Several methods had been proposed in the evaluation and differentiation of disease activity including positron emission tomography and DCE-MRI [65–67]. DWI has been proposed as an alternative for the assessment of disease activity. In a study conducted by Kamper et al. a calculated DWI-index was significantly higher in untreated patients than in patients under therapy [68]. Up to two-thirds of the idiopathic cases of retroperitoneal fibrosis are believed to be associated with IgG4 disease [69, 70]. Imaging findings are characterized by the development of abnormal soft tissue thickening and fat stranding in the retroperitoneum which can be iso- to hypointense on T1W and of variable signal intensity on T2W images, depending on the degree of active inflammation [71]. Three subtypes of retroperitoneal fibrosis are described according to the imaging pattern: (1) Abnormal soft tissue surrounding the abdominal aorta and its branches, (2) periureteral masses often related with hydronephrosis and (3) Plaquelike retroperitoneal mass [69, 70]. Enhancement after contrast administration varies according with the maturity of the fibrous tissue [71].

Conclusion

Technically optimized MRU can be considered an excellent technique for evaluation of the entire urinary tract. The combination of functional sequences with conventional MRU

offers the possibility of a MP-MRI examination, which is the reference standard for renal mass and bladder cancer in clinical practice. The application of motion correction techniques, radiomic features, and incorporation of machine-learning algorithms may further improve examination tolerance and diagnostic efficacy. MRU is the preferred technique for the evaluation of the urinary tract in pediatric patients, individuals with history of severe allergy to iodinated contrast agents or young patients requiring frequent repeated imaging. As future technological developments are implemented into clinical practice we look forward to improved utilization of MRU for many other clinical indications.

References

1. Zeikus E, Sura G, Hindman N, Fielding JR (2018) Tumors of Renal Collecting Systems, Renal Pelvis, and Ureters. Magn Reson Imaging Clin N Am. 27(1):15–32
2. Leyendecker JR, Clingan MJ (2009) Magnetic Resonance Urography Update-Are We There Yet? Semin Ultrasound, CT MRI. 30(4):246–257
3. Silverman SG, Leyendecker JR, Amis ES (2009) What Is the Current Role of CT Urography and MR Urography in the Evaluation of the Urinary Tract? Radiology. 250(2):309–323
4. Potenta SE, D'Agostino R, Sternberg KM, Tatsumi K, Perusse K (2015) CT Urography for Evaluation of the Ureter. Radiographics. 35:709–726
5. Raman SP, Fishman EK (2018) Upper and Lower Tract Urothelial Imaging Using Computed Tomography Urography. Urol Clin North Am. 45(3):389–405
6. Jinzaki M, Kikuchi E, Akita H, et al. (2016) Role of computed tomography urography in the clinical evaluation of upper tract urothelial carcinoma. Int J Urol. 23(4):284–298
7. Razavi SA, Sadigh G, Kelly AM, Cronin P (2012) Comparative Effectiveness of Imaging Modalities for the Diagnosis of Upper and Lower Urinary Tract Malignancy: A Critically Appraised Topic. Acad Radiol. 19(9):1134–1140
8. Sudah M, Masarwah A, Kainulainen S, et al. (2016) Comprehensive MR urography protocol: Equally good diagnostic performance and enhanced visibility of the upper urinary tract compared to triple-phase CT urography. PLoS One. 11(7):1–12
9. Shanbhogue AK, Dilauro M, Schieda N, et al. (2016) MRI Evaluation of the Urothelial Tract: Pitfalls and Solutions. Am J Roentgenol. 207(6):W108–W116
10. Zand KR, Reinhold C, Haider MA, et al. (2007) Artifacts and pitfalls in MR imaging of the pelvis. J Magn Reson Imaging. 26(3):480–497
11. Hamilton J, Franson D, Seiberlich N (2017) Recent advances in parallel imaging for MRI. Prog Nucl Magn Reson Spectrosc. 101:71–95
12. Leyendecker JR, Barnes CE, Zagoria RJ (2008) MR Urography: Techniques and Clinical Applications. RadioGraphics. 28(1):23–46
13. Hoosein MM, Rajesh A (2014) MR imaging of the urinary bladder. Magn Reson Imaging Clin N Am. 22(2):129–134
14. Battal B (2015) Split-bolus MR urography: synchronous visualization of obstructing vessels and collecting system in children. Diagn Interv Radiol. 21:498–502
15. Nolte-ernsting CCA, Adam GB, Günther RW (2001) MR urography : examination techniques and clinical applications. Eur Radiol. 11:355–372
16. Weadock WJ, Korobkin M, Ergen FB, et al. (2007) 3D excretory MR urography: Improved image quality with intravenous saline and diuretic administration. J Magn Reson Imaging. 25(4):783–789
17. Dym RJ, Chernyak V, Rozenblit AM (2013) MR imaging of renal collecting system with gadoxetate disodium: Feasibility for MR urography. J Magn Reson Imaging. 38(4):816–823
18. Moosavi B, Schieda N, Flood TA, McInnes MDF, Ramamurthy NK (2014) Multiparametric MRI of solid renal masses: pearls and pitfalls. Clin Radiol. 70(3):304–316
19. Leyendecker JR, Gianini JW (2009) Magnetic Resonance Urography. Abdom Imaging. 34:527–540
20. Bhargava P, Dighe MK, Lee JH, Wang C (2012) Multimodality Imaging of Ureteric Disease. Radiol Clin North Am. 50(2):271–299
21. Kim S, Jacob JS, Kim DC, et al. (2008) Time-resolved dynamic contrast-enhanced MR urography for the evaluation of ureteral peristalsis: Initial experience. J Magn Reson Imaging. 28(5):1293–1298
22. Yoshida S, Masuda H, Ishii C, et al. (2011) Usefulness of diffusion-weighted MRI in diagnosis of upper urinary tract cancer. Am J Roentgenol. 196(1):110–116
23. Pol CB Van Der, Chung A, Lim C, Gandhi N, Tu W, Mcinnes MDF, et al. Update on Multiparametric MRI of Urinary Bladder Cancer. J Magn Reson Imaging. 2018;1–15.
24. Panebianco V, Narumi Y, Altun E, et al. (2018) Multiparametric Magnetic Resonance Imaging for Bladder Cancer: Development of VI-RADS (Vesical Imaging-Reporting And Data System). Eur Urol. 74(3):294–306
25. Lassel EA, Rao R, Schwenke C, Schoenberg SO, Michaely HJ (2014) Diffusion-weighted imaging of focal renal lesions: A meta-analysis. Eur Radiol. 24(1):241–249
26. Charles-Edwards EM, De Souza NM (2006) Diffusion-weighted magnetic resonance imaging and its application to cancer. Cancer Imaging. 6(1):135–143
27. Maurer MH, Härmä KH, Thoeny H (2018) Diffusion-Weighted Genitourinary Imaging. Urol Clin North Am. 45(3):407–425
28. Qayyum A (2009) Diffusion-weighted Imaging in the Abdomen and Pelvis: Concepts and Applications. RadioGraphics. 29(6):1797–1810
29. Koh Dow-Mu, Collins David J. Diffusion-Weighted MRI in the Body: Applications and Challenges in Oncology. Am J Roentgenol. 2007;188(6):1622–35.
30. Fujii Y, Kihara K, Koga F, Masuda H, Yoshida S (2014) Role of diffusion-weighted magnetic resonance imaging as an imaging biomarker of urothelial carcinoma. Int J Urol. 21(12):1190–1200
31. Okaneya T, Nishizawa S, Kamigaito T, et al. (2010) Diffusion weighted imaging in the detection of upper urinary tract urothelial tumors. Int braz j urol. 36(1):18–28
32. Akita H, Jinzaki M, Kikuchi E, et al. (2011) Preoperative T categorization and prediction of histopathologic grading of urothelial carcinoma in renal pelvis using diffusion-weighted MRI. Am J Roentgenol. 197(5):1130–1136
33. Grant KB, Wood BJ, Agarwal HK, et al. (2014) Comparison of calculated and acquired high b value diffusion-weighted imaging in prostate cancer. Abdom Imaging. 40(3):578–586
34. Rosenkrantz AB, Chandarana H, Hindman N, et al. (2013) Computed diffusion-weighted imaging of the prostate at 3 T: Impact on image quality and tumour detection. Eur Radiol. 23(11):3170–3177
35. Correa AF, Yankey H, Li T, et al. (2019) Renal Hilar Lesions: Biological Implications for Complex Partial Nephrectomy. Urology. 123:174–180
36. Choi K, McCafferty R, Deem S (2017) Contemporary management of upper tract urothelial cell carcinoma. World J Clin Urol. 6(1):1

37. Krishna S, Schieda N, Flood TA, et al. (2018) Magnetic resonance imaging (MRI) of the renal sinus. Abdom Radiol. 43(11):3082–3100
38. Wehrli NE, Kim MJ, Matza BW, et al. (2013) Utility of MRI features in differentiation of central renal cell carcinoma and renal pelvic urothelial carcinoma. Am J Roentgenol. 201(6):1260–1267
39. Schieda N, Davenport MS, Pedrosa I, et al. (2019) Renal and adrenal masses containing fat at MRI: Proposed nomenclature by the society of abdominal radiology disease-focused panel on renal cell carcinoma. J Magn Reson Imaging. 49(4):917–926
40. Schieda, N.; Krishna S, ; Davenport M. Update on Gadolinium-Based Contrast Agent-Enhanced Imaging in the Genitourinary System. Am J Roentgenol. 2019;11:1–11.
41. Flood TA, Shabana WM, Schieda N, et al. (2015) Diagnosis of Sarcomatoid Renal Cell Carcinoma With CT: Evaluation by Qualitative Imaging Features and Texture Analysis. Am J Roentgenol. 204(5):1013–1023
42. Zhang GMY, Sun H, Shi B, Jin ZY, Xue HD (2017) Quantitative CT texture analysis for evaluating histologic grade of urothelial carcinoma. Abdom Radiol. 42(2):561–568
43. Mammen S, Krishna S, Quon M, et al. (2018) Diagnostic Accuracy of Qualitative and Quantitative Computed Tomography Analysis for Diagnosis of Pathological Grade and Stage in Upper Tract Urothelial Cell Carcinoma. J Comput Assist Tomogr. 42(2):204–210
44. Liu ZH, Shi JY, Wang HY, et al. (2018) CT texture analysis in bladder carcinoma: histologic grade characterization. Zhonghua Zhong Liu Za Zhi. 40(5):379–383
45. Lim CS, Tirumani S, van der Pol CB, et al. (2019) Use of Quantitative T2-Weighted and Apparent Diffusion Coefficient Texture Features of Bladder Cancer and Extravesical Fat for Local Tumor Staging After Transurethral Resection. AJR Am J Roentgenol. 12:1–10
46. Patino M, Fuentes JM, Singh S, Hahn PF, Sahani DV (2015) Iterative reconstruction techniques in abdominopelvic CT: Technical concepts and clinical implementation. Am J Roentgenol. 205(1):W19–W31
47. Padole A, Khawaja RDA, Kalra MK, Singh S (2015) CT radiation dose and iterative reconstruction techniques. Am J Roentgenol. 204(4):W384–W392
48. Wu D, Kim K, El Fakhri G, Li Q (2017) Iterative Low-Dose CT Reconstruction With Priors Trained by Artificial Neural Network. IEEE Trans Med Imaging. 36(12):2479–2486
49. McCarthy CJ, Baliyan V, Kordbacheh H, Sajjad Z, Sahani D, Kambadakone A. Radiology of renal stone disease. Int J Surg. 2016;36(PD):638–46.
50. Kalb B, Sharma P, Salman K, et al. (2010) Acute abdominal pain: Is there a potential role for MRI in the setting of the emergency department in a patient with renal calculi? J Magn Reson Imaging. 32(5):1012–1023
51. Eisner BH, McQuaid JW, Hyams E, Matlaga BR (2011) Nephrolithiasis: What surgeons need to know. Am J Roentgenol. 196(6):1274–1278
52. Shokeir AA, El-Diasty T, Eassa W, Mosbah A, El-Ghar MA, Mansour O, et al. Diagnosis of ureteral obstruction in patients with compromised renal function: The role of noninvasive imaging modalities. J Urol. 2004;171(6 I):2303–6.
53. Hiorns MP (2011) Imaging of the urinary tract: The role of CT and MRI. Pediatr Nephrol. 26(1):59–68
54. Roy C, Labani A, Alemann G, et al. (2016) DWI in the Etiologic Diagnosis of Excretory Upper Urinary Tract Lesions: Can It help in Differentiating Benign From Malignant Tumors? A Retrospective Study of 98 Patients. Am J Roentgenol. 207(1):106–113
55. Oh SN, Choi Y-J, Lee JM, Jung SE, Byun JY, Rha SE, et al. The Renal Sinus: Pathologic Spectrum and Multimodality Imaging Approach. RadioGraphics. 2007;24(suppl_1):S117–31.
56. Vikram R, Sandler CM, Ng CS (2009) Imaging and staging of transitional cell carcinoma: part 2, upper urinary tract. AJR Am J Roentgenol. 192(6):1488–1493
57. Vikram R, Sandler CM, Ng CS (2009) Imaging and staging of transitional cell carcinoma: Part 1, lower urinary tract. Am J Roentgenol. 192(6):1481–1487
58. Lee CH, Tan CH, De Castro Faria S, Kundra V (2017) Role of imaging in the local staging of urothelial carcinoma of the bladder. Am J Roentgenol. 208(6):1193–1205
59. Mao Y, Kilcoyne A, Hedgire S, et al. (2016) Patterns of recurrence in upper tract transitional cell carcinoma: Imaging surveillance. Am J Roentgenol. 207(4):789–796
60. Duarte S, Figueiredo F, Cruz J, et al. (2018) Infectious and Inflammatory Diseases of the Urinary Tract. Magn Reson Imaging Clin N Am. 27(1):59–75
61. Cronin CG, Lohan DG, Blake MA, et al. (2008) Retroperitoneal Fibrosis: A Review of Clinical Features and Imaging Findings. Am J Roentgenol. 191(2):423–431
62. Cohan RH, Francis IR, Kaza RK, et al. (2011) Multimodality Imaging in Ureteric and Periureteric Pathologic Abnormalities. Am J Roentgenol. 197(6):W1083–W1092
63. Rajiah P, Sinha R, Cuevas C, et al. (2011) Imaging of Uncommon Retroperitoneal Masses. RadioGraphics. 31(4):949–976
64. Goenka AH, Shah SN, Remer EM (2012) Imaging of the Retroperitoneum. Radiol Clin North Am 50(2):333–355
65. Kamper L, Brandt AS, Scharwächter C, et al. (2011) MR evaluation of retroperitoneal fibrosis. RoFo Fortschritte auf dem Gebiet der Rontgenstrahlen und der Bildgeb Verfahren. 183(8):721–726
66. Vaglio A, Salvarani C, Buzio C (2006) Retroperitoneal fibrosis. Lancet (London, England). 367(9506):241–251
67. Burn PR, Singh S, Barbar S, Boustead G, King CM (2002) Role of gadolinium-enhanced magnetic resonance imaging in retroperitoneal fibrosis. Can Assoc Radiol J. 53(3):168–170
68. Kamper L, Brandt AS, Ekamp H, et al. (2014) Diffusion-weighted MRI findings of treated and untreated retroperitoneal fibrosis. Diagn Interv Radiol. 20(6):459–463
69. Katabathina VS, Khalil S, Shin S, et al. (2016) Immunoglobulin G4-Related Disease: Recent Advances in Pathogenesis and Imaging Findings. Radiol Clin North Am. 54(3):535–551
70. Hedgire SS, McDermott S, Borczuk D, et al. (2013) The spectrum of IgG4-related disease in the abdomen and pelvis. AJR Am J Roentgenol. 201(1):14–22
71. Tan TJ, Ng YL, Tan D, Fong WS, Low ASC (2014) Extrapancreatic findings of IgG4-related disease. Clin Radiol. 69:209–218